2010 IEEE International Conference on Robotics and Automation
Anchorage Convention District
May 3-8, 2010, Anchorage, Alaska, USA

Low-cost Attitude and Heading Reference System: Filter Design and Experimental Evaluation

Pedro Batista, Carlos Silvestre, Paulo Oliveira, and Bruno Cardeira

Abstract— **This paper presents the design and performance evaluation of a low-cost Attitude and Heading Reference System (AHRS) for autonomous vehicles. A single sensor pack, an Inertial Measurement Unit (IMU), provides all the data required to feed the attitude filter. The design is sensor-driven and departs from traditional solutions as no explicit representations of the attitude, e.g., Euler angles, quaternions, or rotation matrices, are considered in the filter design. Moreover, the proposed solution includes the estimation of rate gyros biases, systematic tuning procedures, and also allows for the inclusion of frequency weights to model colored noise on the different sensor channels. Due to its inherent structure, the filter is complementary, allows for temporary loss of sensor measurements, and also copes well with slowly time-varying rate gyros biases. The performance of the proposed algorithm is experimentally evaluated with a low-cost IMU and resorting to a high precision calibration table, which provides ground truth signals for comparison with the resulting filter estimates.**

I. INTRODUCTION

Traditional attitude estimation methods consist, as discussed in the recent survey paper [1], of a two-step process: i) estimate the attitude from body measurements and known reference observations, and ii) filtering the noisy quantities. The first step, where an attitude estimate is obtained from body measurements to feed a filter (or an observer), ends up in one of many known representations, e.g., Euler angles, quaternions, Euler angle-axis representation, rotation matrix, etc. [2]. For the filtering process there is also a very large number of alternatives, depending on the models and representations of the attitude. Kinematic models, which resort basically to three-axis rate gyros, are exact. However, these sensors have nonidealities such as biases, which are often time-varying. Dynamic models for the angular velocity, on the other hand, are usually complex, highly nonlinear, often time-varying, and the mobile platform inertia matrix and angular damping coefficients may not be well known, as well as other dynamic parameters. With all these possible combinations, there are many attitude estimation solutions in the literature. Extended Kalman Filters (EKFs) and some other filtering variants have been widely used, see [3], [4], and [5], for instance. In spite of the good performance achieved by EKF and EKF-like solutions, divergence due to the linearization of the system dynamics [1] has led the scientific community to pursue different solutions, in particular nonlinear observers such as those presented in [6] and [7]. For a more thorough survey, the reader is referred to [1]. In all the aforementioned references, sensors data are essentially used to obtain instantaneous measurements of the attitude that are used afterwards to feed an observer or filter, depending on whether or not a stochastic approach is considered. Sensor specificness is therefore disregarded and, even when it is addressed, the nonlinear transformations that are required to obtain the attitude from vector measurements distort noise characteristics. Moreover, with the exception of EKF and EKF-like solutions, systematic tuning procedures are often absent. Exceptions can be found in [8] and [9] where vector measurements are used directly in the feedback of observers built on the Special Orthogonal Group $SO(3)$ and the Special Euclidean Group $SE(3)$, respectively. In the first local exponential stability is achieved and the error is shown to converge to zero for almost all initial conditions, while in the second case almost global exponential stability (AGES) is shown for the observer error dynamics. In [10] a semiglobal practical asymptotic observer was also proposed for attitude estimation, that preserves orthogonality constraints. Another invariant approach was presented in [11].

This paper presents a novel Attitude and Heading Reference System that

- is based directly on the measurements provided by an Inertial Measurement Unit (IMU);
- resorts to the exact angular motion kinematics;
- builds on the well-established Kalman filtering theory;
- provides systematic filter tuning procedures based directly on the sensor noise characteristics, including frequency weights to model colored noise;
- estimates rate gyros biases and copes well with slowly time-varying biases;
- has a complementary structure, combining low bandwidth vector observations with high bandwidth rate gyro measurements; and
- allows for temporary loss of magnetic field measurements, due to space anomalies.

Most important, the proposed technique does not suffer from singularities, double covering, topological limitations for global asymptotic stabilization, and/or unwinding phenomena as solutions that use attitude representations (Euler angles, quaternions, rotation matrices, etc.) in the filter design do [12]. Instead of using the IMU measurements to build a

The work of P. Batista was supported by a PhD Student Scholarship from the POCTI Programme of FCT, SFRH/BD/24862/2005.

This work was partially supported by Fundação para a Ciência e a Tecnologia (ISR/IST plurianual funding), by the projects PTDC/MAR/64546/2006 - OBSERVFLY of the FCT, and by the EU Project TRIDENT (Contract No. 248497).

The authors are with the Institute for Systems and Robotics, Instituto Superior Técnico, Av. Rovisco Pais, 1049-001 Lisboa, Portugal.
{pbatista,cjs,pjcro,bcardeira}@isr.ist.utl.pt

978-1-4244-5040-4/10/$26.00 ©2010 IEEE

representation of the attitude, the dynamics of the sensor readings are used directly in the filter and the attitude is obtained afterwards, as in traditional solutions, but using filtered estimates of the sensor readings.

Essential to the filter design is a modification of the sensor-based system dynamics that yields a structure that can be regarded as linear time-varying (LTV), although the system still is, in fact, nonlinear. However, the system dynamics are exact and no linearization is performed whatsoever. The Kalman filter design follows for a discrete-time version of the system, and the final attitude estimation solution results from combining the sensor-based filter with an optimal attitude determination algorithm. This last problem is commonly known in the literature as the Wahba's problem [13] and, for two vector observations, there are closed-form solutions available in the literature, see [14], [15], [1], and references therein. Preliminary theoretical work by the authors can be found in [16]. This papers details the AHRS filter design and provides experimental results of the resulting system. The proposed setup has ground truth data available for performance evaluation purposes.

The paper is organized as follows. The sensor-based framework that is the core of the proposed AHRS is presented in Section II. The filter design and overall structure of the AHRS is detailed in Section III, where temporary loss of sensor measurements is also discussed. The performance of the proposed solution is experimentally evaluated in Section IV and Section V summarizes the main contributions and conclusions of the paper.

A. Notation

Throughout the paper the symbol $\mathbf{0}$ denotes a matrix (or vector) of zeros and $\mathbf{I}$ an identity matrix, both of appropriate dimensions. A block diagonal matrix is represented as $\mathrm{diag}(\mathbf{A}_1, \ldots, \mathbf{A}_n)$. If $\mathbf{x}$ and $\mathbf{y}$ are two vectors of identical dimensions, $\mathbf{x} \times \mathbf{y}$ represents the cross product. Finally, the Dirac delta function is denoted by $\delta(t)$.

II. SENSOR-BASED FRAMEWORK

A. Sensor-based Concept

Although many alternative sensing devices may be selected, consider a vehicle equipped with an Inertial Measurement Unit, which contains three triads of orthogonally mounted rate gyros, accelerometers, and magnetometers. The magnetometers provide the magnetic field in body-fixed coordinates. This quantity is locally constant in inertial coordinates and it is therefore a feasible vector observation for attitude estimation, as discussed in [8]. On the other hand, for sufficiently low frequency bandwidths, the gravitational field also dominates the accelerometer measurements, as discussed in [8]. This provides a second vector observation, which is, in general, not parallel to the first. Therefore, it is possible to determine the attitude of the vehicle with an IMU. Fig. 1 depicts a traditional attitude estimation solution. As it is possible to observe, vector measurements such as the gravitational and magnetic fields are first used to compute a representation of the attitude of the vehicle. Afterwards, the attitude filter evolves according to the representation of the attitude and resorting to kinematic or dynamic attitude models. With this classic approach the transformations that

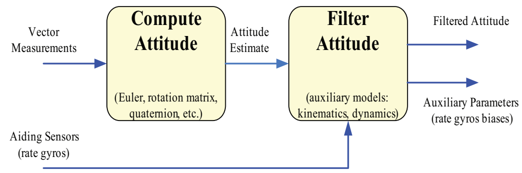

Fig. 1. Classic Attitude Estimation Solution

are necessarily performed to obtain an attitude representation distort the noise characteristics of the signals. Moreover, attitude representations such as Euler angles, quaternions, rotation matrices, etc., have singularities, topological limitations for achieving global asymptotic stability and/or double covering. The core concept of the paper is to take into account the specificness of each sensor by designing the filter directly in the space of the sensors, as exemplified in Fig. 2. An attitude representation, for example a rotation matrix, which does not have singularities and does not exhibit double covering behavior as quaternions do [2], is then obtained from the filtered estimates. In addition to the inclusion of the specificness of the sensors in the filter design, topological restrictions on $SO(3)$ for achieving global asymptotic stability are no longer in place since the filtering process occurs prior to the estimation of the attitude.

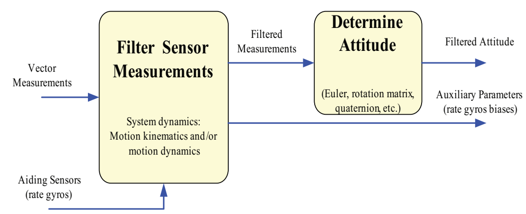

Fig. 2. Sensor-based Attitude Estimation Approach

B. System dynamics

Let $\{I\}$ denote a local inertial frame, $\{B\}$ the body-fixed frame, and $\mathbf{R}(t) \in SO(3)$ the rotation matrix from $\{B\}$ to $\{I\}$. The attitude kinematics are given by $\dot{\mathbf{R}}(t) = \mathbf{R}(t)\mathbf{S}\left[\boldsymbol{\omega}(t)\right]$, where $\boldsymbol{\omega}(t) \in \mathbb{R}^3$ is the angular velocity of $\{B\}$, expressed in $\{B\}$, and $\mathbf{S}\left(\boldsymbol{x}\right)$ is the skew-symmetric matrix such that $\mathbf{S}\left(\boldsymbol{x}\right)\boldsymbol{y} = \boldsymbol{x} \times \boldsymbol{y}$.

For the sake of generality, suppose that non-collinear measurements $\mathbf{y}_1(t) \in \mathbb{R}^3$ and $\mathbf{y}_2(t) \in \mathbb{R}^3$ are available, in body-fixed coordinates, of known constant vectors in inertial coordinates, ${}^I\mathbf{y}_1 = \mathbf{R}(t)\mathbf{y}_1(t)$ and ${}^I\mathbf{y}_2 = \mathbf{R}(t)\mathbf{y}_2(t)$, respectively. Then, the dynamics of $\mathbf{y}_1(t)$ and $\mathbf{y}_2(t)$ are given by

$$\begin{cases} \dot{\mathbf{y}}_1(t) = -\mathbf{S}\left[\boldsymbol{\omega}(t)\right]\mathbf{y}_1(t) \\ \dot{\mathbf{y}}_2(t) = -\mathbf{S}\left[\boldsymbol{\omega}(t)\right]\mathbf{y}_2(t) \end{cases}.$$

Further consider rate gyro measurements $\boldsymbol{\omega}_m(t) \in \mathbb{R}^3$ corrupted with constant bias $\mathbf{b}_{\boldsymbol{\omega}}(t) \in \mathbb{R}^3$, i.e., $\boldsymbol{\omega}_m(t) = \boldsymbol{\omega}(t) + \mathbf{b}_{\boldsymbol{\omega}}(t)$. Then, the system dynamics may be written as

$$\begin{cases} \dot{\mathbf{x}}_1(t) = -\mathbf{S}\left[\boldsymbol{\omega}_m(t)\right]\mathbf{x}_1(t) + \mathbf{S}\left[\mathbf{b}_{\boldsymbol{\omega}}(t)\right]\mathbf{x}_1(t) \\ \dot{\mathbf{x}}_2(t) = -\mathbf{S}\left[\boldsymbol{\omega}_m(t)\right]\mathbf{x}_2(t) + \mathbf{S}\left[\mathbf{b}_{\boldsymbol{\omega}}(t)\right]\mathbf{x}_2(t) \\ \dot{\mathbf{b}}_{\boldsymbol{\omega}}(t) = \mathbf{0} \\ \mathbf{y}_1(t) = \mathbf{x}_1(t) \\ \mathbf{y}_2(t) = \mathbf{x}_2(t) \end{cases}, \quad (1)$$

where the states $\mathbf{x}_1(t)$ and $\mathbf{x}_2(t)$ correspond to the two vector measurements. In the AHRS presented in the paper $\mathbf{y}_1(t)$ corresponds to the magnetic field measurements and $\mathbf{y}_2(t)$ to the gravity field measurements.

III. Attitude and Heading Reference System

The complete design of the proposed Attitude and Heading Reference System is presented in this section. The sensor-based filter is derived in Section III-A, whereas the overall structure of the AHRS is discussed in Section III-B. Finally, temporary loss of magnetic field measurements is addressed in Section III-C.

A. Sensor-Based Filter Design

The system dynamics (1) are nonlinear. Notice, however, that using the cross product property $\boldsymbol{x} \times \boldsymbol{y} = -\boldsymbol{y} \times \boldsymbol{x}$, it is possible to rewrite (1) as

$$\begin{cases} \dot{\mathbf{x}}_1(t) = -\mathbf{S}\left[\boldsymbol{\omega}_m(t)\right]\mathbf{x}_1(t) - \mathbf{S}\left[\mathbf{x}_1(t)\right]\mathbf{b}_{\boldsymbol{\omega}}(t) \\ \dot{\mathbf{x}}_2(t) = -\mathbf{S}\left[\boldsymbol{\omega}_m(t)\right]\mathbf{x}_2(t) - \mathbf{S}\left[\mathbf{x}_2(t)\right]\mathbf{b}_{\boldsymbol{\omega}}(t) \\ \dot{\mathbf{b}}_{\boldsymbol{\omega}}(t) = \mathbf{0} \\ \mathbf{y}_1(t) = \mathbf{x}_1(t) \\ \mathbf{y}_2(t) = \mathbf{x}_2(t) \end{cases}$$

or, in compact form, as

$$\begin{cases} \dot{\boldsymbol{x}}(t) = \mathbf{A}(t)\boldsymbol{x}(t) \\ \mathbf{y}(t) = \mathbf{C}\boldsymbol{x}(t) \end{cases}, \quad (2)$$

where

$$\mathbf{A}(t) = \begin{bmatrix} -\mathbf{S}\left[\boldsymbol{\omega}_m(t)\right] & \mathbf{0} & -\mathbf{S}\left[\mathbf{y}_1(t)\right] \\ \mathbf{0} & -\mathbf{S}\left[\boldsymbol{\omega}_m(t)\right] & -\mathbf{S}\left[\mathbf{y}_2(t)\right] \\ \mathbf{0} & \mathbf{0} & \mathbf{0} \end{bmatrix}$$

and

$$\mathbf{C} = \begin{bmatrix} \mathbf{I} & \mathbf{0} & \mathbf{0} \\ \mathbf{0} & \mathbf{I} & \mathbf{0} \end{bmatrix}.$$

Now, although the system dynamics (2) are nonlinear, they may, nevertheless, be regarded as LTV. Moreover, it was shown in [16] that the system is uniformly completely observable provided that the vector observations are not parallel. This is an important result that leads naturally to the design of a Kalman filter with globally asymptotically stable error dynamics, see [16].

In practice, and although there are commercial off-the-shelf IMUs that provide continuous-time signals, these are usually sampled and the AHRS core algorithm is implemented in a digital setup. Therefore, it is convenient to derive a discrete-time solution. To that purpose, let T_s denote the sampling period of the IMU measurements. Then, ignoring sensor noise for now, let the discrete-time measurements be given by $\boldsymbol{\omega}_m(k) := \boldsymbol{\omega}_m(t_k),\ t_k = kT_s + t_0,\ k \in \mathbb{N}_0$, and $\mathbf{y}_i(k) := \mathbf{y}_i(t_k),\ t_k = kT_s + t_0,\ k \in \mathbb{N}_0,\ i \in \{1, 2\}$, where t_0 is the initial time. The Euler discretization of the system dynamics (2) gives

$$\begin{cases} \boldsymbol{x}(k+1) = \boldsymbol{x}(k) + T_s\mathbf{A}(t_k)\boldsymbol{x}(k) \\ \mathbf{y}(k+1) = \mathbf{C}\boldsymbol{x}(k+1) \end{cases},$$

Including system disturbances and sensor noise, the discrete-time dynamics read as

$$\begin{cases} \mathbf{x}(k+1) = \mathbf{A}_d(k)\mathbf{x}(k) + \mathbf{w}(k) \\ \mathbf{y}(k+1) = \mathbf{C}\mathbf{x}(k+1) + \mathbf{n}(k+1) \end{cases}, \quad (3)$$

where

$$\mathbf{A}_d(k) = \mathbf{I} - T_s \begin{bmatrix} \mathbf{S}\left[\boldsymbol{\omega}_m(k)\right] & \mathbf{0} & \mathbf{S}\left[\mathbf{y}_1(k)\right] \\ \mathbf{0} & \mathbf{S}\left[\boldsymbol{\omega}_m(k)\right] & \mathbf{S}\left[\mathbf{y}_2(k)\right] \\ \mathbf{0} & \mathbf{0} & \mathbf{0} \end{bmatrix},$$

$\mathbf{w}(k) = \left[\mathbf{w}_1^T(k)\ \mathbf{w}_2^T(k)\ \mathbf{w}_3^T(k)\right]^T \in \mathbb{R}^9$ is zero-mean, discrete-time, white Gaussian noise, with $\mathrm{E}\left[\mathbf{w}(\mathrm{k})\mathbf{w}^{\mathrm{T}}(\mathrm{j})\right] = \boldsymbol{\Xi}(\mathrm{k})\delta(\mathrm{k}-\mathrm{j})$, $\mathbf{n}(k) = \left[\mathbf{n}_1^T(k)\ \mathbf{n}_2^T(k)\right]^T \in \mathbb{R}^6$ is zero-mean, discrete-time, white Gaussian noise, with $\mathrm{E}\left[\mathbf{n}(\mathrm{k})\mathbf{n}^{\mathrm{T}}(\mathrm{j})\right] = \boldsymbol{\Theta}(\mathrm{k})\delta(\mathrm{k}-\mathrm{j})$, and $\mathrm{E}\left[\mathbf{w}(\mathrm{k})\mathbf{n}^{\mathrm{T}}(\mathrm{j})\right] = \mathbf{0}$. Notice that, for filtering design purposes, both $\mathbf{w}$ and $\mathbf{n}$ could have been modeled as the outputs of stable discrete-time linear time invariant filters, which could be easily employed to model, e.g., colored noise, see [17] for an example of such application. In this paper, and for the sake of clarity of presentation, the simplest white Gaussian noise version is presented. The Kalman filter equations for the system dynamics (3) are standard [18], [19] and therefore omitted.

It is important to stress that the resulting structure is complementary: high bandwidth rate gyro measurements are combined with low bandwidth vector observations to determine a low frequency perturbation in the gyro measurements and provide filtered estimates of the vector observations. Moreover, as the bias is assumed to be driven by white Gaussian noise, it is possible to cope well with slowly time-varying bias.

Remark 1: One should notice that additive Gaussian noise may not be the best modeling option. Indeed, multiplicative noise would do a better job, as the presence of noise in the gyro measurements is reflected as terms like $T_s\mathbf{S}\left[\mathbf{w}_i(k)\right]\mathbf{x}_i(k),\ i = 1, 2$, instead of simple additive system disturbances. Also, different noise distributions could better model the sensors noise. As an alternative, it is possible to consider $\mathbf{w}(k) \in \mathcal{L}_2$ and $\mathbf{n}(k) \in \mathcal{L}_2$, where $\mathcal{L}_2$ denotes the space of square integrable signals, and design an $\mathcal{H}_\infty$ filter instead of a Kalman filter. The steps are similar and therefore will be omitted.

B. AHRS Structure

The final Attitude and Heading Reference System results from combining the sensor-based filter with an algorithm that determines the proper rotation matrix $\hat{\mathbf{R}}(t_k) \in SO(3)$ which best explains the vector estimates provided by the filter. The problem of finding the proper rotation matrix $\mathbf{R}(t_k)$ that minimizes the loss function

$$J(\mathbf{R}(t_k)) = \frac{1}{2}\sum_{i=1}^{N} a_i \left\|\mathbf{y}_i(t_k) - \mathbf{R}^T(t_k)\,{}^I\mathbf{y}_i\right\|^2,\ a_i > 0,$$

is known in the literature as the Wahba's problem [13]. Although the first solution dates from 1966, extensive research has been carried out throughout the years and there exist nowadays a rather large variety of solutions, see [20] for a thorough survey.

In the previous section a Kalman filter was derived that yields filtered estimates $\hat{\mathbf{y}}_1(t_k)$ and $\hat{\mathbf{y}}_2(t_k)$ of the vector observations $\mathbf{y}_1(t_k)$ and $\mathbf{y}_2(t_k)$ provided by the triad of accelerometers and magnetometers. Instead of using the sensor measurements, the filtered estimates are normalized,

$$\hat{\mathbf{y}}_1^u(t_k) = \frac{\hat{\mathbf{y}}_1(t_k)}{\|\hat{\mathbf{y}}_1(t_k)\|},\ \hat{\mathbf{y}}_2^u(t_k) = \frac{\hat{\mathbf{y}}_2(t_k)}{\|\hat{\mathbf{y}}_2(t_k)\|},$$

as well as the corresponding inertial vectors,

$${}^I\mathbf{y}_1^u = \frac{{}^I\mathbf{y}_1}{\|{}^I\mathbf{y}_1\|},\ {}^I\mathbf{y}_2^u = \frac{{}^I\mathbf{y}_2}{\|{}^I\mathbf{y}_2\|},$$

and the attitude matrix is reconstructed using the closed-loop (and computationally efficient) optimal solution presented in [15], that minimizes

$$J\left(\hat{\mathbf{R}}(t_k)\right) = \frac{1}{2}\sum_{i=1}^{2} a_i \left\|\hat{\mathbf{y}}_i^u(t_k) - \hat{\mathbf{R}}^T(t_k)\,{}^I\mathbf{y}_i^u\right\|^2,$$

and that is omitted here due to the lack of space and as it can be found in [15]. The coefficients a_i can be chosen to reflect the confidence on each sensor.

Remark 2: There is nothing in the filter structure imposing any particular constraint on $\hat{\mathbf{y}}_1(t_k)$ or $\hat{\mathbf{y}}_2(t_k)$. Therefore, it may happen, due to bad initialization or by accident, that $\hat{\mathbf{y}}_1(t_k)$ and $\hat{\mathbf{y}}_2(t_k)$ are parallel or null for some time t_k. In this case, the optimal solution presented in [15] is not well defined. If any of these situations happens, the sensor measurements could be used directly to obtain an estimate of the attitude. However, notice that the filter may be initialized with the first set of vector observations. In addition to that, it will be shown shortly that the filter convergence, which is global, is very fast, and warming-up delays below $1\,\mathrm{s}$ are achieved. Therefore, none of these situations are likely to happen in practice.

C. Temporary Loss of Sensor Measurements

It is well known that, for two nonparallel vector observations, the attitude is uniquely determined, and for a single vector observation, it is impossible to determine the complete attitude. However, there is still some interest in the study of this case. Dead-reckoning navigation systems such as Inertial Navigation Systems (INS) provide open-loop propagation of the motion state. The estimation of the position and attitude of the vehicle is necessarily obtained in this type of systems by integrating higher-order derivatives such as the linear acceleration and the angular velocity. As such, and regardless of the accuracy and precision of the IMU, the errors in the position and attitude estimates grow unbounded due to the noise and bias of the sensors [21]. A single vector observation does not provide the entire attitude but it may help compensating for the bias and restricting the attitude uncertainty to a set of lower dimension. For example, gravitational field measurements yield the bank and elevation angles.

While for classic AHRS the loss of one vector observation is not trivially accounted for, as the filter algorithm usually requires the entire attitude representation, that is not the case of the present solution. Indeed, if there is a temporary loss of, e.g., magnetic field measurements due to space anomalies, the state corresponding to the magnetic field can be simply propagated in open-loop using the rate-gyro measurements corrected with the bias estimate. The remaining system dynamics stay untouched, which still allows for the estimation of rate gyros biases under some mild observability conditions, see [16] for further details. Therefore, the proposed AHRS also provides a simple way to deal with temporary loss of magnetic field measurements.

IV. Experimental Evaluation

A. Experimental Setup

In order to evaluate the performance in real world applications, an experimental setup was developed resorting to a high precision calibration table, Model 2103HT from Ideal Aerosmith [22], which allows for accurate and reliable motion control. The table outputs, in a fixed-frequency profile mode, the angular position of the table with a resolution of $0.00025\,°$, considered as a ground truth signal. The IMU that was employed is the nanoIMU NA02-0150F50 [23], from MEMSENSE, which outputs data at a rate of $150\ \mathrm{Hz}$. This 9 degree-of-freedom (DOF) Micro-Electro-Mechanical System (MEMS) device is a miniature, light weight, 3-D digital output sensor (it outputs 3-D acceleration, 3-D angular rate, and 3-D magnetic field data) featuring RS422 or I2C protocols, with built-in bias, sensitivity, and temperature compensation. The standard deviations of the noise of the outputs of the IMU are $0.0015\,\mathrm{G}$ and $0.008\,\mathrm{m/s^2}$ for the magnetometers and accelerometers, respectively, and $0.95\,°/s$ for the rate gyros. These low-grade specifications correspond to the worst case standard deviation values provided by the manufacturer. Fig. 3 displays the calibration table with the experimental setup mounted on the table top. The nIMU is interfaced through the RS422 bus to a PC104 card that logs all the generated data in a solid state disk.

Fig. 3. Experimental setup

Unfortunately, the calibration table distorts the magnetic field in the neighborhood of the IMU, even though it was attempted to place the IMU as far as possible from the rest of the experimental setup, by means of a small nonmagnetic bar, which elevates the sensor from the table top. Therefore, magnetic field measurements were simulated in the loop. Sensor noise was naturally added so that the results are as realistic as possible.

B. Performance Evaluation

The real-time performance of the AHRS is evaluated in this section. The Motion Rate Table introduced in Section IV-A has three rotational joints which allow for movement about 3 orthogonally mounted axis, so called inner, middle, and outer axis, and that were defined as the x, y, and z axis of the body-fixed reference frame, so that the rotation from body-fixed coordinates to inertial coordinates is given by

$$\mathbf{R}(t) = \mathbf{R}_z\left(\theta_{out}(t)\right)\mathbf{R}_y\left(\theta_{mid}(t)\right)\mathbf{R}_x\left(\theta_{inn}(t)\right),$$

where $\mathbf{R}_x(.)$, $\mathbf{R}_y(.)$, and $\mathbf{R}_z(.)$ are the rotation matrices about the x, y, and z axis, respectively, and θ_{inn}, θ_{mid}, and θ_{out} are the inner, middle, and outer axis angles, respectively. The evolution of the inner, middle, and outer angles is depicted in Fig. 4. Notice that the angular motion full range is used, and if Euler angles were employed problems would have appeared due to singularities. Also, note that the angular velocity $\boldsymbol{\omega}(t)$, which is shown in Fig. 5, reaches interesting values, typical of many autonomous vehicles such as Autonomous Underwater Vehicles, Autonomous Ground Vehicles, or Unmanned Air Vehicles.

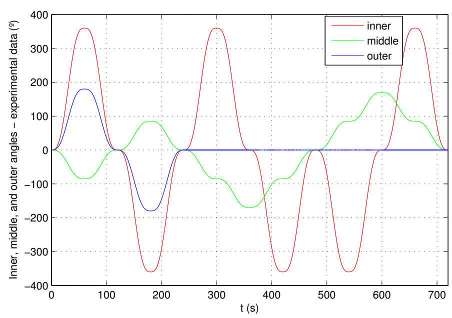

Fig. 4. Evolution of the inner, middle, and outer angles

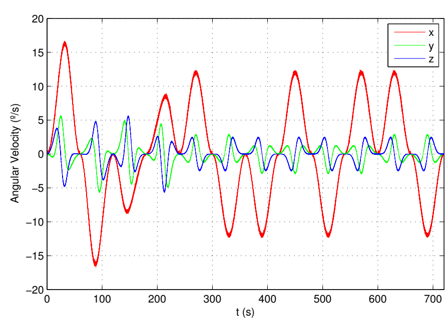

Fig. 5. Evolution of the angular velocity $\boldsymbol{\omega}(t)$

The sampling rate of the system is 150 Hz. The Kalman filter parameters were set according to the sensor noise levels and sampling rate,

$$\boldsymbol{\Xi} = 0.5\mathrm{diag}\left(\frac{1}{150}0.0015\mathbf{I}, \frac{1}{150}0.008\mathbf{I}, 2\times10^{-8}\mathbf{I}\right)$$

and $\boldsymbol{\Theta} = \mathrm{diag}\left(0.0015\mathbf{I}, 0.008\mathbf{I}\right)$. No particular emphasis was given on the tuning process as the resulting performance with these simple parameters is very good. In practice, the spectral contents of the sensors noise may be experimentally approximated and frequency weights adjusted to improve the performance of the filter, see the examples provided in [17]. Moreover, correlation between the system disturbances $\mathbf{w}$ and the sensor noise $\mathbf{n}$ may also be considered. Since $\mathbf{x}_1$ and $\mathbf{x}_2$ are measured, the corresponding estimates were initialized with the first set of measurements. The initial bias estimate was set to zero.

The convergence rate of the filter is very fast and the steady-state is achieved in less than 1 s. The initial evolution of the error variables is not show due to the lack of space. The steady-state evolution of the filter error is depicted in Fig. 6. The filtering performance is evident by comparison with the noise standard deviation of the corresponding sensors.

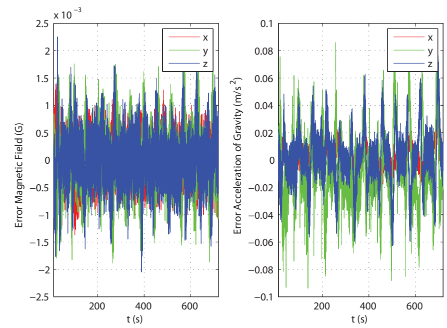

Fig. 6. Detailed evolution of the filter error

Since it is not possible to plot the evolution of the bias error, as the true bias is unknown, Fig. 7 displays the steady-state evolution of the bias estimate. As it can be seen, the rate gyros biases estimates changes slowly over time, which is quite typical of low-cost units.

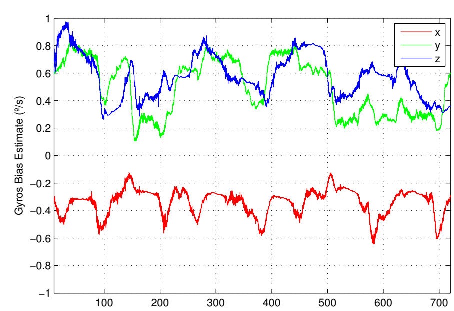

Fig. 7. Detailed evolution of the rate gyros biases estimates

In order to evaluate the overall attitude performance, yaw, pitch, and roll Euler angles could have been computed from the estimated rotation matrix. However, as these would have singularities due to the full-range trajectory described by the platform, and for the purpose of performance evaluation only, an additional error variable is defined as

$$\tilde{\mathbf{R}}(t) = \mathbf{R}^T(t)\hat{\mathbf{R}}(t),$$

which corresponds to the rotation matrix error. Using the Euler angle-axis representation for this new error variable, the evolution of the angle error is shown in Fig. 8. The mean error is $0.125\,^\circ$, which is a very good value considering the low-grade specifications of the IMU at hand. It is also comparable with the results obtained in simulation, which are not shown on the paper due to space limitations. In comparison with built-in commercial of-the-shelf solutions, the AHRS 3DM-GX1, from MicroStrain, provides an attitude with a standard deviation error of $2\,^\circ$. At the same time, the noise levels of the sensors of the IMU considered in this paper are at least twice of those of Microstrain, according to the manufacturers specifications. Further improvements could be achieved by analyzing the spectral contents of the sensor measurements at rest and including the sensor frequency response specifications in the filter design.

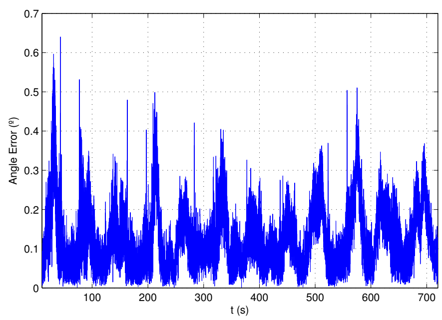

Fig. 8. Evolution of the attitude estimation error using an Euler angle-axis representation

V. Conclusions

This paper presented the design and performance evaluation of a sensor-based Attitude and Heading Reference System for autonomous vehicles. Traditional solutions typically ignore the specificness of the sensors and have drawbacks such as singularities, double-covering, ad-hoc tuning procedures, and/or topological limitations for achieving global asymptotic stabilization. The proposed solution, which is based directly on the measurements provided by an Inertial Measurement Unit, includes the estimation of rate gyro biases, systematic tuning procedures, and also allows for the inclusion of frequency weights to model colored noise on the different sensor channels. Due to its inherent structure, the filter is complementary, allows for temporary loss of sensor measurements, and also copes well with slowly time-varying rate gyro biases. Finally, it is also independent of the particular mobile platform dynamics as it relies solely on kinematic models, which are exact. The performance of the AHRS was evaluated with an experimental setup that includes a high precision Motion Rate Table. This table provided ground truth signals in order to assess the performance of the resulting AHRS, which was shown to be very good in spite of the specifications of the low-cost IMU that was used in the tests.

Acknowledgments

The authors gratefully acknowledge the expertise and contributions of Luís Sebastião, André Oliveira, and José Tojeira in the development of the experimental setup.

References

[1] J. Crassidis, F. Markley, and Y. Cheng, “Survey of Nonlinear Attitude Estimation Methods,” *Journal of Guidance, Control and Dynamics*, vol. 30, no. 1, pp. 12–28, Jan.-Feb. 2007.

[2] M. Shuster, “A Survey of Attitude Representations,” *Journal of the Astronautical Sciences*, vol. 41, no. 4, pp. 439–517, Oct.-Dec. 1993.

[3] J. Farrell, “Attitude Determination by Kalman Filter,” *Automatica*, vol. 6, no. 5, pp. 419–430, 1970.

[4] I. Bar-Itzhack and Y. Oshman, “Attitude Determination from Vector Observations: Quaternion Estimation,” *IEEE Transactions on Aerospace and Electronic Systems*, vol. 321, no. 1, pp. 128–136, Jan. 1985.

[5] A. Sabatini, “Quaternion-based extended Kalman filter for determining orientation by inertial and magnetic sensing,” *IEEE Transactions on Biomedical Engineering*, vol. 53, no. 7, pp. 1346–1356, Jul. 2006.

[6] J. Thienel and R. Sanner, “A Coupled Nonlinear Spacecraft Attitude Controller and Observer With an Unknown Constant Gyro Bias and Gyro Noise,” *IEEE Transactions on Automatic Control*, vol. 48, no. 11, pp. 2011–2015, Nov. 2003.

[7] H. Rehbinder and B. Ghosh, “Pose Estimation Using Line-Based Dynamic Vision and Inertial Sensors,” *IEEE Transactions on Automatic Control*, vol. 48, no. 2, pp. 186–199, Feb. 2003.

[8] R. Mahony, T. Hamel, and J.-M. Pflimlin, “Nonlinear Complementary Filters on the Special Orthogonal Group,” *IEEE Transactions on Automatic Control*, vol. 53, no. 5, pp. 1203–1218, Jun. 2008.

[9] J. Vasconcelos, R. Cunha, C. Silvestre, and P. Oliveira, “Landmark Based Nonlinear Observer for Rigid Body Attitude and Position Estimation,” in *Proceedings of the 46th IEEE Conference on Decision and Control*, New Orleans, LA, USA, Dec. 2007, pp. 1033–1038.

[10] D. Laila, M. Lovera, and A. Astolfi, “A numerical algorithm as an observer for spacecraft attitude determination,” in *Proceedings of the 45th IEEE Conference on Decision and Control*, San Diego, CA, USA, Dec. 2006, pp. 1568–1573.

[11] P. Martin and E. Salaun, “Invariant observers for attitude and heading estimation from low-cost inertial and magnetic sensors,” in *Proceedings of the 46th IEEE Conference on Decision and Control*, New Orleans, LA, USA, Dec. 2007, pp. 1039–1045.

[12] D. Bernstein and S. Bhata, “A topological obstruction to continuous global stabilization of rotational motion and the unwinding phenomenon,” *Systems & Control Letters*, vol. 39, no. 1, pp. 63–70, 2000.

[13] G. Wahba, “A Least Squares Estimate of Spacecraft Attitude,” *SIAM Review*, vol. 7, no. 3, p. 409, Jul. 1965.

[14] M. Shuster and S. Oh, “Three-Axis Attitude Determination from Vector Observations,” *Journal of Guidance, Control and Dynamics*, vol. 4, no. 1, pp. 70–77, Jan.-Feb. 1981.

[15] F. Markley, “Optimal Attitude Matrix from Two Vector Measurements,” *Journal of Guidance, Control and Dynamics*, vol. 31, no. 3, pp. 765–768, May-June 2008.

[16] P. Batista, C. Silvestre, and P. Oliveira, “Sensor-based Complementary Globally Asymptotically Stable Filters for Attitude Estimation,” in *Proceedings of the 48th IEEE Conference on Decision and Control*, Shanghai, China, Dec. 2009, pp. 7563–7568.

[17] ——, “Position and Velocity Navigation Filters for Marine Vehicles,” in *Proceedings of the 17th IFAC World Congress*, Seoul, Korea, Jul. 2008, pp. 15 016–15 021.

[18] R. Kalman and R. Bucy, “New Results in Linear Filtering and Prediction Theory,” *Transactions of the ASME - Journal of Basic Engineering, Series D*, vol. 83, no. 3, pp. 95–108, Mar. 1961.

[19] A. G. (Ed), *Applied Optimal Filtering*. The MIT Press, 1974.

[20] F. Markley and D. Mortari, “How to Estimate Attitude from Vector Observations,” *Proceedings of the AAS/AIAA Astrodynamics Specialist Conference*, vol. 103, no. 3, pp. 1979–1996, Aug. 1999.

[21] M. Bryson and S. Sukkarieh, “Vehicle Model Aided Inertial Navigation for a UAV using Low-Cost Sensors,” in *Proceedings of the 2004 Australasian Conference on Robotics and Automation*, Canberra, Australia, Dec. 2004.

[22] Ideal Aerosmith, Inc., “2103HT Multi-Axis Table Data Sheet, Rev C,” http://www.ideal-aerosmith.com/, 2006.

[23] MEMSENSE, “NANO IMU Product Specification User’s Guide, Document Number PSD-0822, Rev. A,” ”http://www.memsense.com”, 2009.